

# **Preserving Neuromuscular Synapses in ALS by Stimulating MuSK with a Therapeutic Agonist Antibody**

Sarah Cantor<sup>1\*</sup>, Wei Zhang<sup>1</sup>, Nicolas Delestrée<sup>2</sup>, Leonor Remédio<sup>1</sup>, George Z. Mentis<sup>2</sup>, and Steven J. Burden<sup>1\*</sup>

- 1 Molecular Neurobiology Program  
Helen L. and Martin S. Kimmel Center for Biology and Medicine  
at the Skirball Institute of Biomolecular Medicine  
NYU Medical School  
540 First Avenue  
New York, NY 10016  
Tel.: 212-263-7341  
FAX: 212-263-2842
  
- 2 Center for Motor Neuron Biology and Disease & Departments of  
Pathology and Cell Biology and Neurology  
Columbia University  
630 W 168<sup>th</sup> Street  
New York, NY 10032

Running title: Preserving neuromuscular synapses in ALS

Corresponding Author and Lead Contact: [steve.burden@med.nyu.edu](mailto:steve.burden@med.nyu.edu)

## Summary

In amyotrophic lateral sclerosis (ALS) and animal models of ALS, including *SOD1-G93A* mice, disassembly of the neuromuscular synapse precedes motor neuron loss and is sufficient to cause a decline in motor function that culminates in lethal respiratory paralysis. We treated *SOD1-G93A* mice with an agonist antibody to MuSK, a receptor tyrosine kinase essential for maintaining neuromuscular synapses, to determine whether increasing muscle retrograde signaling would slow nerve terminal detachment from muscle. The agonist antibody, delivered after disease onset, slowed muscle denervation, promoting motor neuron survival, improving motor system output, and extending the lifespan of *SOD1-G93A* mice. These findings suggest a novel therapeutic strategy for ALS, using an antibody format with clinical precedence, which targets a pathway essential for maintaining attachment of nerve terminals to muscle.

Key words: MuSK, agonist antibody, denervation, amyotrophic lateral sclerosis, neuromuscular disease, motor neuron, neurodegeneration

## Introduction

Amyotrophic lateral sclerosis (ALS) is a neurodegenerative disease that progresses relentlessly from a subtle decline in motor function to lethal respiratory paralysis within a few years of diagnosis (1, 2). The disease can be familial and caused by dominant mutations in one of several genes, including *SOD1*, *C9orf72*, *TDP43*, and *FUS* (2). More commonly, however, the disease is idiopathic.

Although motor neuron cell death is a hallmark feature of ALS, the loss of neuromuscular synapses occurs prior to the loss of motor neurons and is the primary cause of motor paralysis in both familial and sporadic forms of ALS (3-5). The detachment of motor nerve terminals and withdrawal of motor axons has received less attention than the later loss of motor neurons, but therapeutic approaches designed to preserve neuromuscular synapses have the potential to maintain motor function, especially during the early phases of disease, and provide benefit to the quality of life for patient and family.

Transgenic mice bearing dominant mutations in the human *SOD1* gene, including *SOD1-G93A* mice, recapitulate the hallmark features of

ALS and provide the most thoroughly studied animal model for ALS (6, 7). Moreover, because detachment of motor nerve terminals is the primary cause for paralysis in *SOD1-G93A* mice, *SOD1-G93A* mice represent a clinically relevant model for ALS.

The signaling pathways that control attachment of motor axon terminals to muscle are only beginning to be understood, but two genes, *Lrp4* and *Musk*, expressed by muscle, play important roles. *Lrp4*, a member of the LDL receptor family, is the muscle receptor for the critical neuronal ligand, Agrin (8, 9). Upon binding Agrin, *Lrp4* associates with MuSK, a receptor tyrosine kinase, stimulating MuSK and leading to anchoring and enhanced expression of critical postsynaptic proteins, including *Lrp4* (10). Clustered *Lrp4* then signals back to motor axons to stimulate their attachment and differentiation (11).

Recessive mutations in *Agrin*, *Lrp4* or *Musk* cause congenital myasthenia, a group of neuromuscular disorders, distinct from ALS, which compromise the structure and function of neuromuscular synapses and lead to muscle weakness and fatigue (12). Moreover, autoantibodies

to Agrin, Lrp4, or MuSK cause myasthenia gravis (MG), which is likewise distinct from ALS (13). In MuSK MG, the pathogenic antibodies are usually directed to the first Ig-like domain in MuSK and reduce MuSK phosphorylation by impairing binding between Lrp4 and MuSK (14, 15).

Although defects in the MuSK signaling pathway are not associated with ALS, increasing *MuSK* gene expression stabilizes neuromuscular synapses in *SOD1-G93A* mice, reducing the extent of muscle denervation and improving motor function (16). However, these experiments used transgenic mice to modestly increase *MuSK* expression from muscle, beginning during early development, several months prior to disease onset. Therefore, the therapeutic potential of increasing MuSK signaling as a strategy to reduce denervation and improve motor function in patients diagnosed with ALS remained unclear. Here, we sought to determine whether a pharmacological approach to increase MuSK activity *in vivo* would preserve neuromuscular synapses in *SOD1-G93A* mice when dosing was initiated after disease onset. This type of approach would have substantially

improved potential for translation to ALS patients without the complex requirements for gene therapy (17).

## **Results**

### **Agonist antibodies to MuSK**

A previous study identified twenty-one single chain antibodies (scFvs) that recognize mouse MuSK and raised the idea that a subset of these antibodies may function as MuSK agonists *in vivo* (18). We studied the activity of two antibodies, #13 and #22, reported to stimulate MuSK in cultured myotubes, as well as antibody #21, reported to bind but not stimulate MuSK. We confirmed that antibodies #13 and #22, re-engineered as human IgG1 molecules, stimulated MuSK tyrosine phosphorylation in the C2 mouse muscle cell line (Figure 1A), whereas antibody #21, as well as a control IgG1 antibody to ragweed pollen, failed to stimulate MuSK phosphorylation (Figure 1A).

Agrin stimulates MuSK phosphorylation by binding Lrp4, which promotes association between Lrp4 and MuSK, requiring the first of three Ig-like domains in MuSK (19). In contrast to the Agrin-dependent mechanism for activating MuSK, the agonist antibody binds the Fz-like

domain in MuSK, force-dimerizing and stimulating MuSK phosphorylation, independent of Lrp4 (Figures 1B, C, S1). Importantly, the Fz-like domain is dispensable for synapse formation in mice (20).

### **MuSK agonist antibodies engage MuSK *in vivo***

To determine whether agonist antibody #13 could engage MuSK *in vivo*, we intraperitoneally (IP) injected varying amounts of the MuSK agonist antibody on a human IgG1 backbone, or a control human IgG1 antibody to ragweed pollen, into wild-type mice. Several days later, we stained whole mounts of the diaphragm muscle to determine whether the agonist antibody engaged MuSK at the synapse. Figure 2A shows that neuromuscular synapses were labeled specifically by the MuSK agonist antibody. MuSK staining was evident as early as 3-days (Figure 2A, iv-vi), and staining persisted for at least 7-days after the single injection (Figure 2A, vii-ix). The organization of AChRs and nerve terminals appeared normal (Figure 2A, ii, v, viii), indicating that the MuSK agonist antibody did not disturb major features of synaptic differentiation. Moreover, visual observation of the antibody-injected mice did not reveal overt behavioral abnormalities, indicating that the

MuSK agonist antibody was well tolerated by the mice. Two mg/kg of the agonist antibody was sufficient to saturate MuSK labeling at the synapse (Figure 2B) and increase MuSK tyrosine phosphorylation *in vivo* (Figure 1-figure supplement 1).

We measured the pharmacokinetic properties of the injected antibody and found that the half-life of the injected antibody in blood was ~12 days (Figure 2C). The antibody exhibited linear clearance for 21 days after antibody injection, indicating that exposure could be maintained over several weeks. In addition, these results demonstrated that the mouse immune system did not recognize and clear the antibody, which contained a human Fc region, from the circulation over this three-week time period (Figure 2C).

### **Single dose of MuSK agonist antibody decreases denervation in *SOD1-G93A* mice**

We studied female and male *SOD1-G93A* mice, on a C57BL/6 background, with 21-26 copies of the human *SOD1-G93A* gene (Figure 3-figure supplement 1). In *SOD1-G93A* mice, denervation of limb muscles begins at P50, whereas denervation of the diaphragm muscle

begins a month later (5, 21). Because denervation of the diaphragm muscle is responsible for lethal respiratory paralysis, we focused our analysis on innervation of this muscle. We first quantified the extent of innervation in the diaphragm muscle at P90 by staining for nerve terminals and postsynaptic AChRs, which remain even at denervated synaptic sites (Figure 3A). Denervation was evident in *SOD1-G93A* mice as early as P90 (Figure 3B, C). From P90 to P110, the extent of full innervation, defined as perfect apposition of nerve terminals and the AChR-rich postsynaptic membrane, decreased from 77.3% to 18.1% in female and from 53.1% to 16.1% in male *SOD1-G93A* mice (Figure 3B). Likewise, the extent of complete denervation increased from 2.3% to 41% in female and from 16.7% to 24.4% in male *SOD1-G93A* mice over this twenty-day period (Figure 3C).

*SOD1-G93A* mice were injected with the MuSK agonist antibody at P90. Because the antibody had a half-life of 12-days and 2mg/kg of antibody saturated MuSK at the synapse (Figure 2 B, C), we injected *SOD1-G93A* mice with 10mg/kg of agonist antibody, ensuring that the antibody concentration in blood would remain at saturating levels for

MuSK-binding over the 20-day period. We found that a single dose of the MuSK agonist antibody increased the number of fully innervated synapses by 2.7- and 2.5-fold in female and male *SOD1-G93A* mice, respectively, and decreased the number of fully denervated synapses by 3.7- and 2.3-fold in female and male *SOD1-G93A* mice, respectively (Figure 3B, C). These findings demonstrated that the MuSK agonist antibody, introduced after disease onset, decreased motor axon withdrawal from the diaphragm muscle.

### **Chronic dosing with the MuSK agonist antibody halts further denervation in *SOD1-G93A* mice for over two months**

To determine whether the MuSK agonist antibody could preserve neuromuscular synapses over a longer time period, we chronically dosed *SOD1-G93A* mice. To avoid host recognition and clearance of the antibody during chronic exposure, we used a MuSK #13 antibody on a murine IgG2a backbone that also lacked effector functions (22). The ability of this ‘reverse chimera’ to bind and stimulate MuSK was similar to the antibody with a human IgG backbone (Figure 4-figure supplement

1). Moreover, the ‘reverse chimera’ had a half-life similar to the human agonist antibody *in vivo* (Figure 4-figure supplement 2).

*SOD1-G93A* mice were injected with 10mg/kg of the reverse chimera agonist antibody at P90 and every 24 days thereafter, and we sacrificed chronically injected mice every 24 days to quantify innervation of the diaphragm muscle (Figure 4A). Because 2mg/kg of antibody saturated MuSK at the synapse and because the antibody had a 11 day half-life in blood, this dosing schedule ensured that saturating levels of the MuSK agonist antibody were maintained at all times (Figure 4-figure supplement 2).

In *SOD1-G93A* mice injected with a control antibody to GP120, synaptic loss continued to decline from P114 through P162, so that only 11% of the synapses were fully innervated at P162 (Figure 4B). This progressive loss was halted by injection of the MuSK agonist antibody, as the number of fully innervated synapses was largely unchanged (40-50%) from P114 to P162 in *SOD1-G93A* mice injected with the MuSK agonist antibody (Figure 4B). Similarly, the number of fully denervated synapses continued to increase from P114 through P162 in *SOD1-G93A*

mice injected with the control antibody, whereas this progressive increase was prevented by the MuSK agonist antibody (Figure 4C). These findings indicate that the MuSK agonist antibody prevented further synaptic loss and preserved synapses for at least 50 days after signs of denervation and disease were evident in *SOD1-G93A* mice.

During disease progression, synapses transition through a partially innervated phase, when only a portion of the AChR-rich postsynaptic membrane is apposed by motor nerve terminals (Figure 4-figure supplement 3). Although the number of partially innervated synapses was similar in *SOD1-G93A* mice injected with the control or MuSK agonist antibody (Figure 4-figure supplement 3), the extent of nerve terminal coverage was 34% greater at partially innervated synapses in mice injected with the MuSK agonist antibody (Figure 4-figure supplement 3). Thus, the MuSK agonist antibody increased both full innervation as well as nerve terminal coverage at partially innervated synapses in *SOD1-G93A* mice.

### **Improved motor system output of the diaphragm muscle**

To determine whether maintaining neuromuscular synapses led to improved motor system output, we used an *ex-vivo* phrenic nerve/diaphragm muscle preparation to measure the compound muscle action potentials (CMAPs), following phrenic nerve stimulation. We studied *SOD1-G93A* mice three to four weeks prior to end-stage (Figure 5). We stimulated the phrenic nerve to the diaphragm muscle and recorded CMAPs, which elicit muscle contraction (Figure 5-figure supplement 1). We found no significant difference in the amplitude of the first CMAP between *SOD1 G93A* mice injected with the MuSK agonist antibody or the control antibody to GP120 (anti-GP120-treated males:  $5.95 \pm 1.14 \text{mV}$ ; anti-MuSK-treated males:  $5.93 \pm 0.52 \text{mV}$ ; anti-GP120-treated females:  $4.95 \pm 0.54 \text{mV}$ ; anti-MuSK-treated females:  $5.81 \pm 0.63 \text{mV}$ ). We next measured the reliability of synaptic transmission at the neuromuscular junction by repetitively stimulating the phrenic nerve at a physiological frequency (20Hz). We found a rapid and severe decline in the amplitude of the CMAP, indicative of synaptic dysfunction and denervation, in *SOD1-G93A* mice chronically injected with the

control antibody to GP120. In contrast, the decline in CMAP amplitude was far less severe in *SOD1 G93A* mice treated with the MuSK agonist antibody, demonstrating that the MuSK agonist antibody improved neuromuscular function (Figure 5). Moreover, repetitive stimulation of the phrenic nerve at a more challenging frequency (50Hz) led to frequent failures to elicit a CMAP in *SOD1-G93A* mice injected with the control antibody to GP120. Such failures were less frequent in *SOD1-G93A* mice injected with the MuSK agonist antibody, similar to wild-type mice (Figure 5). These CMAP failures are likely due to presynaptic mechanisms, such as conduction block or impaired neurotransmitter release, rather than the inability of motor end plates to generate an action potential. In either case, the maintenance of neuromuscular synapses, stimulated by the MuSK agonist antibody, led to improved reliability of synaptic transmission and output of the critically important diaphragm muscle in *SOD1-G93A* mice.

**MuSK agonist antibody decreases motor neuron loss in *SOD1-G93A* mice**

We next assessed whether preserving neuromuscular synapses in *SOD1-G93A* mice reduced motor neuron death. During embryonic development motor neuron death is regulated by innervation and reduced when motor neurons make additional synapses with muscle (23-25), whereas survival of adult motor neurons is less dependent upon muscle innervation (26). We quantified the number of motor neurons, stained for choline acetyltransferase (ChAT), in the lumbar spinal cord of *SOD1-G93A* mice injected chronically either with the control antibody to GP120 or the MuSK agonist antibody (Figure 6A). The MuSK agonist antibody increased the number of motor neurons by 31 to 57% at P138 (Figure 6B), during the peak period of motor neuron cell death in *SOD1-G93A* mice when approximately half of spinal motor neurons have been lost (6). These findings demonstrate that increasing retrograde signaling after disease onset not only preserves neuromuscular synapses but also promotes survival of spinal motor neurons in *SOD1-G93A* mice.

### **MuSK agonist antibody extends lifespan of *SOD1-G93A* mice**

Denervation of the diaphragm muscle is responsible for lethal respiratory paralysis in *SOD1-G93A* mice and ALS. We therefore asked whether maintaining neuromuscular synapses and improving output of the diaphragm muscle extended the lifespan of *SOD1-G93A* mice. Female *SOD1-G93A* mice injected with the control antibody to GP120 had an average lifespan of 169 days (see Materials and methods), whereas male *SOD1-G93A* mice injected with the control antibody had an average lifespan of 157.5 days (Figure 6C, D). Chronic injection with the MuSK agonist antibody prolonged survival of female and male *SOD1-G93A* mice by 7 ( $p < 0.05$ ) and 10 days ( $p < 0.001$ ), respectively (Figure 6C, D). Thus, the MuSK agonist antibody, introduced after disease onset, slowed the disassembly of neuromuscular synapses, improved motor output of the diaphragm muscle and extended the lifespan of *SOD1-G93A* mice.

## **Discussion**

ALS is a devastating disease that progresses in a relentless manner from detachment of motor nerve terminals to lethal respiratory paralysis within several years of diagnosis. Currently, there is an unmet need for

therapies that significantly alter the course of disease. Here, we describe a therapeutic approach designed to slow the loss of motor innervation to muscle by targeting a well-defined molecule and mechanism for forming and maintaining neuromuscular synapses. We show that an agonist antibody to MuSK, introduced after disease onset, decreases muscle denervation, improves motor system output, reduces motor neuron loss and extends survival in an aggressive mouse model of ALS. If this strategy, described here for an aggressive mouse model of ALS, were similarly successful in preserving innervation in sporadic and familial ALS, this therapeutic approach would have the potential to improve the quality of life for ALS patients, and as such warrants further study.

Anti-sense RNA directed toward *SOD1* is currently being tested as a promising therapeutic for ALS caused by mutations in *SOD1* (27). A similar approach may ultimately be effective for other dominant, familial forms of ALS (28, 29). However, >80% of ALS patients are diagnosed with sporadic ALS, so strategies to inactivate a single culprit gene are not tenable for most cases of ALS. Instead, multiple, concurrent therapeutic interventions that effectively address the pathology and

symptoms of ALS will likely be necessary to alter the course of disease (30).

Because synaptic loss and muscle denervation are common to sporadic as well as familial forms of ALS, the approach described here has the potential to be effective for both forms of ALS. Moreover, increasing MuSK activity and retrograde signaling may also slow the deterioration of neuromuscular synapses in other neuromuscular diseases and during aging (12, 13, 31, 32). Consistent with this idea, adenoviral expression of Dok-7, an inside-outside activator of MuSK, not only extends longevity of *SOD1 G93A* mice but also provides benefit in other mouse models of neuromuscular disease, including congenital myasthenia and Emery-Dreifuss muscular dystrophy (17, 33). Further, there is increasing evidence that synaptic loss occurs early during disease progression in other neurodegenerative diseases, such as Alzheimer's disease, Huntington's disease, Parkinson's disease and Frontotemporal dementia and Spinal Muscular Atrophy (34), so similar strategies, designed to preserve synapses, may slow progression in these diseases as well.

Our proof of concept experiments were designed to determine whether boosting retrograde signaling *in vivo* with the MuSK agonist antibody might slow motor axon withdrawal and muscle denervation in *SOD1 G93A* mice. As such, we introduced the MuSK agonist antibody after denervation was already evident, during the early phase of denervation in female *SOD1-G93A* mice and mid-phase in male *SOD1-G93A* mice, but before *SOD1 G93A* mice exhibited overt and severe deficits in limb motor function. This timing for delivery of the MuSK agonist antibody may be pertinent and significant for ALS, as denervation is the cause of muscle fibrillations, an early clinical sign in ALS. Because MuSK-dependent retrograde signaling is likely to act focally on nerve terminals and axons that are near the postsynaptic membrane and to be less effective in promoting regeneration of axons that have fully withdrawn, early delivery of a MuSK agonist is likely to be more effective than later delivery in ALS.

However, ALS is a diagnosis of exclusion, leading to delays in diagnosis. Nonetheless, even at late stages of disease, a majority of synapses in *SOD1-G93A* mice are partially innervated, and the MuSK

agonist antibody improved nerve terminal coverage at these partially innervated synapses. These findings suggest that the MuSK agonist antibody may also be effective if introduced later during disease. However, because overt motor deficits become evident in *SOD1-G93A* mice only a month before death, this aggressive mouse model of ALS may not be the optimal and most informative model to infer whether later introduction of the MuSK agonist antibody can stabilize synapses and slow motor dysfunction in ALS.

The loss of motor neurons during embryonic development is regulated, at least in part by synapse formation (23-25). The increased survival of motor neurons in MuSK agonist antibody-injected *SOD1-G93A* mice indicates that adult motor neurons can likewise receive trophic support from muscle. Thus, preserving neuromuscular synapses not only maintains the essential attachment of nerve to muscle but also provides the added benefit of promoting motor neuron survival.

Although we used an agonist antibody to MuSK to stimulate retrograde signaling from muscle, one can envisage other approaches to stimulate MuSK or enhance retrograde signaling in order to maintain

attachment of motor axons to muscle. The MuSK agonist antibody is effective at maintaining neuromuscular synapses in *SOD1 G93A* mice up to P162, but within the next week, synapses are lost, and the mice die. Because the MuSK agonist antibody is designed to maintain neuromuscular synapses and does not directly target or address the underlying cause of the disease and other pathologies in *SOD1 G93A* mice and ALS, the benefit of increasing retrograde signaling from muscle to nerve and promoting nerve terminal attachment is limited. Nonetheless, although the antibody cannot override the many pathological pathways that occur in the motor neuron and in non-neuronal cells, this therapeutic approach has a potent effect on the course of disease, reducing synaptic loss, improving motor output and extending the lifespan of *SOD1-G93A* mice longer than riluzole, the long-standing FDA approved treatment for ALS (35). Motor neuron cell death is a critical feature in ALS, but elimination of Bax, which prevents apoptotic cell death, fails to preserve neuromuscular synapses and increases survival of *SOD1-G93A* mice by only 20 days (36). Together with our studies, these findings give credence to the idea that

combinatorial therapeutic interventions, including those that preserve neuromuscular synapses, will be necessary to fully address the complex pathology and symptoms of ALS and contribute to an improved quality of life for patient and family.

## **Materials and Methods**

### **Study Design**

The investigators were blinded from knowing whether mice were treated with the MuSK agonist or control antibody while acquiring and initially analyzing data. Data are presented as mean  $\pm$  SEM. Statistical comparisons between groups were analyzed using an unpaired, two-tailed Student's *t*-test, log-rank test (survival), linear regression (CMAPs), or two-way ANOVA (failures). Statistical analyses were conducted using Prism 7.0 software (GraphPad Software). The number (n) of mice used to calculate the mean, SEM values and the confidence limits (p values) are indicated in the figure legends.

### **Mice**

The copy number of the human *SOD1-G93A* gene was routinely quantified by TaqMan real-time PCR and normalized to GAPDH (Life

Technologies Assay# Mm00186822\_cn). All mice included in this study had 21-26 copies of *hSOD1-G93A* (Figure 3-figure supplement 1). DietGel 76A (ClearH<sub>2</sub>O) was placed on the cage floor so that mice had ready access to nourishment. Others have measured the lifespan *SOD1 G93A* mice by placing mice on their side and sacrificing mice if they were unable to right themselves in 15 seconds. Because we were concerned that this assay reported on limb muscle function and may not be temporally aligned with the time of death, we used a variant assay, which provided an accurate measure of longevity. When mice were unable to right themselves to eat or drink over the course of several hours, they invariably succumbed within a day; we defined this time as disease end-point and sacrificed mice at this time. Mice were housed and maintained according to Institutional Animal Use and Care Committee (IACUC) guidelines.

## **Histology**

Diaphragm muscles were stained with Alexa 594-conjugated  $\alpha$ -bungarotoxin ( $\alpha$ -BGT) (Life Technologies, Carlsbad, CA) to mark

AChRs and rabbit antibodies to Neurofilament-L (SYnaptic Systems, Goettingen, Germany) and Synapsin 1/2 (SYnaptic Systems, Goettingen, Germany) to label axons and nerve terminals, as described previously (37, 38). At fully innervated synapses, nerve terminal staining completely overlapped with postsynaptic AChRs, whereas nerve terminals were absent from original synaptic sites, marked by AChRs, at fully denervated synapses. At partially innervated synapses, nerve terminals occupied only a portion of the postsynaptic membrane. We examined a minimum of 50 synapses in the diaphragm muscle from each mouse and designated each synapse as fully innervated, partially innervated, or fully denervated. At each partially innervated synapse, the percentage of AChR-stained postsynaptic membrane that was apposed by Synapsin-stained nerve terminals was quantified using Volocity imaging software (PerkinElmer, Waltham, MA). To visualize and quantify staining of the agonist antibody, containing human Fc, at the neuromuscular junction, we used an Alexa 647-conjugated anti-human secondary (Life Technologies, Carlsbad, CA). Whole mounts of muscles

were imaged with a Zeiss LSM800 confocal microscope, and the fluorescent signal was quantified as described previously (37, 38).

Spinal cords were dissected from mice perfused with 4% formaldehyde. Frozen sections (20 $\mu$ m) of the lumbar region were stained with antibodies to choline acetyltransferase (ChAT) (AB144P-200UL from Millipore, Billerica, MA). We defined motor neurons as cells in the ventral horn of the lumbar spinal cord that were positive for ChAT, excluding ChAT-positive preganglionic and Pitx2-positive neurons. We only counted ChAT-stained cells with a clearly defined nucleus in order to avoid double-counting motor neurons in multiple sections. We analyzed ~10 sections, evenly spaced in the lumbar enlargement, which together contained >50 motor neurons in each mouse.

### **Antibody-binding and MuSK phosphorylation**

Chimeric antibodies were produced by transferring cDNAs encoding the variable regions of MuSK agonist antibody #13 to expression vectors containing the mouse kappa and IgG2a constant region. MuSK agonist antibodies were produced in CHO cells and purified by Protein A and

size exclusion chromatography. The activity of the reverse chimera antibody for stimulating clustering of AChRs in C2 myotubes was similar to that for the human agonist antibody to MuSK (Figure 4-figure supplement 1). Fab fragments were prepared by protease digestion of human IgG1 followed by removal of uncleaved IgG and Fc fragments on a Protein A Sepharose column and size exclusion chromatography.

We used a solid-phase binding assay to measure binding between the MuSK agonist antibody and the extracellular (ecto) region (E22 to T494), the first three Ig-like domains (E22 to I103) or the Frizzled-like domain (D312 to K456) from mouse MuSK (19). Maxisorp plates were coated with MuSK agonist antibody #13 (5 $\mu$ g/ml), and subsequently incubated with 8-His-tagged MuSK proteins, followed by a horseradish peroxidase (HRP) conjugated antibody to 8-His. Bound HRP was quantified by measuring HRP activity (Thermo scientific#34028).

C2C12 muscle cells were purchased from the ATCC and were not tested for mycoplasma prior to use. These C2C12 cells, as well as immortalized wild-type or *Lrp4* mutant muscle cells, were differentiated and treated with either neural Agrin (1nM) or antibodies (10nM). MuSK

was immunoprecipitated from lysates, and MuSK expression and MuSK tyrosine phosphorylation were measured by probing Western blots, as described previously (39). C2C12 cells were grown in 24-well culture plates in DMEM with 10% fetal bovine serum (FBS) until myoblasts were 70% confluent. Myoblasts were then allowed to differentiate into myotubes by replacing the FBS with 2% horse serum. After 7 days, the cultures were treated for 16 hr with varying concentrations of rcMuSK antibody #13 or a Fab from antibody MuSK #13. Cells were fixed in 4% paraformaldehyde and stained with Alexa 488 conjugated-  $\alpha$ -BGT. Two to four images were collected from each well, and the number of AChR clusters was analyzed using imageJ software. Neural Agrin (10nM) (R&D Systems, Minneapolis, MN) was used as a positive control for AChR clustering (data not shown).

Hind-limb muscles were denervated by cutting the sciatic nerve, as described previously (40). Four days after denervation, mice were injected with MuSK agonist antibody #13, and we measured MuSK expression and MuSK tyrosine phosphorylation 3 days later. MuSK and Dok-7 were immunoprecipitated from lysates, and their expression

levels were determined by Western blotting (39, 41). MuSK tyrosine phosphorylation was measured by probing Western blots with antibody 4G10, as described previously (39, 41).

### **Recording and evaluation of compound muscle action potentials (CMAPs) from the diaphragm muscle**

To assess the function of neuromuscular junction in the mouse diaphragm muscle (Figure 5-figure supplement 1), we developed an *ex vivo* phrenic nerve-diaphragm preparation. We studied the diaphragm muscle from ~P140 male and ~P150 female mice, which is three to four weeks prior to end-stage, respectively. We did not use the *in vivo* preparation, described by others (42), because we were concerned that *in vivo* stimulation of the phrenic nerve, at moderate to high frequencies, would lead to variable and unreliable CMAP recordings, likely due to changes in the electrode position caused by muscle contraction. Moreover, a related method, reported to record from the mouse diaphragm muscle, uses a surface recording electrode, and likely monitors the activity of multiple thoracic muscles (43). Thus, following anesthesia with 5% isoflurane, mice were decapitated, and the

diaphragm muscle, together with the phrenic nerve, was quickly isolated and transferred to a customized recording chamber. The chamber was perfused continuously with oxygenated (95% O<sub>2</sub> and 5% CO<sub>2</sub>) artificial cerebrospinal fluid solution (128.25mM NaCl, 4mM KCl, 0.58mM NaH<sub>2</sub>PO<sub>4</sub>, 21mM NaHCO<sub>3</sub>, 30mM D-glucose, 1.5mM CaCl<sub>2</sub>, and 1mM MgSO<sub>4</sub>) at a rate of ~10 ml/min at room temperature (~20-24°C). The phrenic nerve that innervates the left hemi-diaphragm muscle was stimulated by drawing the distal part of the left phrenic nerve into a suction electrode (Figure 5-figure supplement 1). We validated proper positioning of the stimulating electrode by visually inspecting muscle contractions following stimulation of the phrenic nerve. EMG activity was recorded using a suction electrode placed in the upper left quadrant of the muscle, 1 mm toward the costal side of the main intramuscular nerve and endplate zone in the middle of the muscle. A light suction was applied to the recording electrode to secure a tight seal between the tip of the electrode and the muscle fibers. In this manner, damage to the diaphragm muscle was avoided, which was confirmed by observing muscle contractions during stimulation. The phrenic nerve was

stimulated with square pulses (0.2ms in duration) at several frequencies (1Hz to 50Hz) for 60sec. The intensity of stimulation was progressively increased from the threshold, defined as the minimum response in three out of five trials, until the CMAP reached a maximal response.

The stimulation intensity was set at twice the intensity required for the maximal response to ensure a supra-maximal intensity of stimulation (25 $\mu$ A to 200 $\mu$ A). Recordings were accepted for analysis only when the CMAP amplitude (peak-to-peak) was unchanged following 1Hz stimulation. The amplitudes of the evoked CMAPs at higher frequencies were expressed as a percentage of the 1<sup>st</sup> evoked CMAP for the entire duration of stimulation. Recordings were fed to an A/D interface (Digidata 1440A, Molecular Devices) and acquired with Clampex (v10.2, Molecular Devices) at a sampling rate of 50kHz. Data were analyzed off-line using Clampfit (v10.2, Molecular Devices). We defined CMAP failures as the absence of an evoked response discernable from the background noise recorded prior to the stimulation.

### **Author Contributions**

S.C., W.Z. L.R. and N.D. designed, performed and interpreted experiments. S.J.B. and G.Z.M. helped to design and interpret experiments. J.L. organized the production and quality control of the MuSK agonist and control antibodies. The manuscript was written by all authors.

## **Acknowledgements**

We are grateful to Martin Raff, Ruth Lehmann and Maartje Huijbers for their comments on the manuscript. We thank Richard Scheller and Jagath Junutula at Genentech for their assistance and commitment in resuscitating the agonist antibodies described here. We thank Joseph Lewcock, Gai Ayalon, Arundhati Sengupta Ghosh and Isidro Hotzel at Genentech for providing the MuSK agonist antibodies as well as the control antibodies to ragweed pollen and GP120 and for *in vitro* data. We thank Elena Michaels for her assistance with confocal microscopy and colony maintenance, and Yonglei Shang for his assistance with the antibody-binding assays. We are grateful to Fernando Vieira and Valerie Tassinari at ALSTDI for their assistance with the qPCR assay for measuring *SOD1-G93A* copy number. This work was supported with funds from the NIH (R37 NS36193), the Robert Packard Center for ALS Research, the ALS Association, and Above and Beyond LLC to SJB and with support from the NIH (RO1NS078375) to GZM. S.C is grateful for support from the Molecular, Cellular, and Translational Neuroscience Training Grant (NIH NINDS, T32 NS86750).

## References

1. P. Pasinelli, R. H. Brown, Molecular biology of amyotrophic lateral sclerosis: insights from genetics. *Nat Rev Neurosci* **7**, 710-723 (2006).
2. J. P. Taylor, R. H. Brown, Jr., D. W. Cleveland, Decoding ALS: from genes to mechanism. *Nature* **539**, 197-206 (2016).
3. L. R. Fischer *et al.*, Amyotrophic lateral sclerosis is a distal axonopathy: evidence in mice and man. *Experimental neurology* **185**, 232-240 (2004).
4. A. M. Schaefer, J. R. Sanes, J. W. Lichtman, A compensatory subpopulation of motor neurons in a mouse model of amyotrophic lateral sclerosis. *The Journal of comparative neurology* **490**, 209-219 (2005).
5. S. Pun, A. F. Santos, S. Saxena, L. Xu, P. Caroni, Selective vulnerability and pruning of phasic motoneuron axons in motoneuron disease alleviated by CNTF. *Nat Neurosci* **9**, 408-419 (2006).
6. S. Vinsant *et al.*, Characterization of early pathogenesis in the SOD1(G93A) mouse model of ALS: part II, results and discussion. *Brain Behav* **3**, 431-457 (2013).
7. S. Vinsant *et al.*, Characterization of early pathogenesis in the SOD1(G93A) mouse model of ALS: part I, background and methods. *Brain Behav* **3**, 335-350 (2013).
8. N. Kim *et al.*, Lrp4 is a receptor for Agrin and forms a complex with MuSK. *Cell* **135**, 334-342 (2008).
9. B. Zhang *et al.*, LRP4 serves as a coreceptor of agrin. *Neuron* **60**, 285-297 (2008).
10. S. J. Burden, N. Yumoto, W. Zhang, The role of MuSK in synapse formation and neuromuscular disease. *Cold Spring Harb Perspect Biol* **5**, a009167 (2013).
11. N. Yumoto, N. Kim, S. J. Burden, Lrp4 is a retrograde signal for presynaptic differentiation at neuromuscular synapses. *Nature* **489**, 438-442 (2012).

12. A. G. Engel, X. M. Shen, D. Selcen, S. M. Sine, Congenital myasthenic syndromes: pathogenesis, diagnosis, and treatment. *Lancet Neurol* **14**, 420-434 (2015).
13. N. E. Gilhus, J. J. Verschuuren, Myasthenia gravis: subgroup classification and therapeutic strategies. *Lancet Neurol* **14**, 1023-1036 (2015).
14. M. G. Huijbers *et al.*, MuSK IgG4 autoantibodies cause myasthenia gravis by inhibiting binding between MuSK and Lrp4. *Proc Natl Acad Sci U S A* **110**, 20783-20788 (2013).
15. I. Koneczny, J. Cossins, P. Waters, D. Beeson, A. Vincent, MuSK myasthenia gravis IgG4 disrupts the interaction of LRP4 with MuSK but both IgG4 and IgG1-3 can disperse preformed agrin-independent AChR clusters. *PLoS One* **8**, e80695 (2013).
16. M. J. Perez-Garcia, S. J. Burden, Increasing MuSK activity delays denervation and improves motor function in ALS mice. *Cell Rep* **2**, 497-502 (2012).
17. S. Miyoshi *et al.*, DOK7 gene therapy enhances motor activity and life span in ALS model mice. *EMBO Mol Med* **9**, 880-889 (2017).
18. M. H. Xie, J. Yuan, C. Adams, A. Gurney, Direct demonstration of MuSK involvement in acetylcholine receptor clustering through identification of agonist ScFv. *Nat Biotechnol* **15**, 768-771 (1997).
19. W. Zhang, A. S. Coldefy, S. R. Hubbard, S. J. Burden, Agrin binds to the N-terminal region of Lrp4 protein and stimulates association between Lrp4 and the first immunoglobulin-like domain in muscle-specific kinase (MuSK). *J Biol Chem* **286**, 40624-40630 (2011).
20. L. Remedio *et al.*, Diverging roles for Lrp4 and Wnt signaling in neuromuscular synapse development during evolution. *Genes Dev* **30**, 1058-1069 (2016).
21. M. C. Rocha, P. A. Pousinha, A. M. Correia, A. M. Sebastiao, J. A. Ribeiro, Early changes of neuromuscular transmission in the SOD1(G93A) mice model of ALS start long before motor symptoms onset. *PLoS One* **8**, e73846 (2013).
22. M. Lo *et al.*, Effector-attenuating Substitutions That Maintain Antibody Stability and Reduce Toxicity in Mice. *J Biol Chem* **292**, 3900-3908 (2017).

23. M. Hollyday, V. Hamburger, Reduction of the naturally occurring motor neuron loss by enlargement of the periphery. *The Journal of comparative neurology* **170**, 311-320 (1976).
24. H. Tanaka, L. T. Landmesser, Cell death of lumbosacral motoneurons in chick, quail, and chick-quail chimera embryos: a test of the quantitative matching hypothesis of neuronal cell death. *J Neurosci* **6**, 2889-2899 (1986).
25. L. Landmesser, The relationship of intramuscular nerve branching and synaptogenesis to motoneuron survival. *J Neurobiol* **23**, 1131-1139 (1992).
26. M. B. Lowrie, G. Vrbova, Dependence of postnatal motoneurons on their targets: review and hypothesis. *Trends Neurosci* **15**, 80-84 (1992).
27. T. M. Miller *et al.*, An antisense oligonucleotide against SOD1 delivered intrathecally for patients with SOD1 familial amyotrophic lateral sclerosis: a phase 1, randomised, first-in-man study. *Lancet Neurol* **12**, 435-442 (2013).
28. L. V. Reddy, T. M. Miller, RNA-targeted Therapeutics for ALS. *Neurotherapeutics* **12**, 424-427 (2015).
29. B. van Zundert, R. H. Brown, Jr., Silencing strategies for therapy of SOD1-mediated ALS. *Neurosci Lett* **636**, 32-39 (2017).
30. R. H. Brown, A. Al-Chalabi, Amyotrophic Lateral Sclerosis. *N Engl J Med* **377**, 162-172 (2017).
31. G. Valdez, J. C. Tapia, J. W. Lichtman, M. A. Fox, J. R. Sanes, Shared resistance to aging and ALS in neuromuscular junctions of specific muscles. *PLoS One* **7**, e34640 (2012).
32. J. E. Poort, M. B. Rheuben, S. M. Breedlove, C. L. Jordan, Neuromuscular junctions are pathological but not denervated in two mouse models of spinal bulbar muscular atrophy. *Hum Mol Genet* **25**, 3768-3783 (2016).
33. S. Arimura *et al.*, Neuromuscular disease. DOK7 gene therapy benefits mouse models of diseases characterized by defects in the neuromuscular junction. *Science* **345**, 1505-1508 (2014).

34. C. M. Henstridge, E. Pickett, T. L. Spires-Jones, Synaptic pathology: A shared mechanism in neurological disease. *Ageing Res Rev* **28**, 72-84 (2016).
35. M. R. Jablonski *et al.*, Inhibiting drug efflux transporters improves efficacy of ALS therapeutics. *Ann Clin Transl Neurol* **1**, 996-1005 (2014).
36. T. W. Gould *et al.*, Complete dissociation of motor neuron death from motor dysfunction by Bax deletion in a mouse model of ALS. *J Neurosci* **26**, 8774-8786 (2006).
37. A. Jaworski, S. J. Burden, Neuromuscular synapse formation in mice lacking motor neuron- and skeletal muscle-derived Neuregulin-1. *J Neurosci* **26**, 655-661 (2006).
38. M. B. Friese, C. S. Blagden, S. J. Burden, Synaptic differentiation is defective in mice lacking acetylcholine receptor beta-subunit tyrosine phosphorylation. *Development* **134**, 4167-4176 (2007).
39. R. Herbst, S. J. Burden, The juxtamembrane region of MuSK has a critical role in agrin-mediated signaling. *EMBO J* **19**, 67-77 (2000).
40. A. M. Simon, P. Hoppe, S. J. Burden, Spatial restriction of AChR gene expression to subsynaptic nuclei. *Development* **114**, 545-553 (1992).
41. P. T. Hallock *et al.*, Dok-7 regulates neuromuscular synapse formation by recruiting Crk and Crk-L. *Genes Dev* **24**, 2451-2461 (2010).
42. A. C. Lepore *et al.*, Human glial-restricted progenitor transplantation into cervical spinal cord of the SOD1 mouse model of ALS. *PLoS One* **6**, e25968 (2011).
43. M. Martin, K. Li, M. C. Wright, A. C. Lepore, Functional and morphological assessment of diaphragm innervation by phrenic motor neurons. *J Vis Exp*, e52605 (2015).

## Figure Legends

**Figure 1. MuSK agonist antibodies activate MuSK, independent of Lrp4, by binding the Fz-like domain in MuSK.** (A) C2 myotubes were treated with neural Agrin or antibodies for the indicated times. MuSK was immunoprecipitated, and Western blots were probed for MuSK or phosphotyrosine. Neural Agrin and MuSK antibodies #13 and #22 stimulate MuSK tyrosine phosphorylation in C2 myotubes, whereas MuSK antibody #21 and a control antibody to Ragweed pollen (Rw) failed to stimulate MuSK phosphorylation. (B) We used a solid-phase binding assay to measure binding of His-tagged MuSK proteins to microtiter wells coated with MuSK agonist antibody #13. The scatter plot shows that full-length ecto-MuSK (■), as well as the MuSK Fz-like domain alone (●) bind MuSK antibody #13 in a dose-dependent and saturable manner; in contrast, the first three Ig-like domains in MuSK (▲) fail to bind the MuSK agonist antibody (n=3). (C) Wild type and *Lrp4* mutant myotubes were treated with neural Agrin or MuSK agonist antibody #13. Agrin stimulates MuSK phosphorylation in wild type but not *Lrp4* mutant myotubes, whereas MuSK agonist antibody #13

stimulates MuSK phosphorylation in both wild type and *Lrp4* mutant myotubes.

**Figure 2. MuSK agonist antibody #13 engages MuSK at the synapse shortly after IP injection.** (A) Staining for the injected MuSK antibody (10mg/kg) was evident as early as three days (iv-vi) and persisted for at least seven days after a single injection of antibody (vii-ix). A human antibody to Ragweed (Rw) pollen (10mg/kg) failed to stain synapses (i-iii) (scale bar=20 $\mu$ m). (B) 2mg/kg of the injected MuSK agonist antibody saturated MuSK at the synapse. The ratio of MuSK/AChR staining at 2mg/kg antibody was assigned a value of 1.0 ( $\pm$  SEM, n=3), and the values at other doses were expressed relative to this value. (C) Following a single injection of human MuSK antibody #13 (10mg/kg) the level of antibody in serum declines with a half-life of 12.1 days. n = 3.

**Figure 3. A single injection of the MuSK agonist antibody at P90 reduced synaptic loss for twenty days in *SOD1-G93A* mice.** (A) AChRs are concentrated in the postsynaptic membrane at innervated and fully denervated synapses (scale bar=20 $\mu$ m). (B, C) Denervation is

evident in female and extensive in male *SOD1-G93A* mice at P90 (▲). Over the next twenty days, the extent of full denervation increases and the number of fully innervated synapses decreases (●). A single injection of agonist antibody #13 (■) reduces the extent of denervation and the loss of innervation. The scatter plot shows the values for individual mice (n = 4 or 5), as well as the mean values and SEM; \*\* p<0.01, \*\*\*\* p<0.0001.

**Figure 4. Chronic dosing with the MuSK agonist antibody prevents further denervation in *SOD1-G93A* mice.** (A) The reverse chimera MuSK agonist antibody #13 was injected at P90 (▲) and every twenty-four days thereafter. (B) The extent of full innervation decreases progressively from P90 to P162 in female and male *SOD1-G93A* injected with a control antibody to GP120 (●). The reverse chimera MuSK agonist antibody #13 (■) halts this progressive loss, as the number of fully innervated synapses is unchanged between P114 and P162. (C) Full denervation increases progressively from P90 to P162 in female and male *SOD1-G93A* injected with a control antibody to GP120 (●). The reverse chimera MuSK agonist antibody #13 prevents this

progressive increase in denervation, as the number of fully denervated synapses is unchanged between P114 and P162 (■). At disease end-stage, the number of fully innervated and denervated synapses was identical in *SOD1-G93A* mice injected with the MuSK agonist or control antibody. The scatter plot shows the values for individual mice (n = 3 to 8), as well as the mean values and SEM; \* p<0.05, \*\*\* p<0.001, \*\*\*\* p<0.0001.

**Figure 5. The MuSK agonist antibody improves motor system output in the diaphragm muscle.** (A,B) 20Hz stimulation (arrow) of the phrenic nerve from *SOD1-G93A* mice injected with the control antibody to GP120 led to a rapid and severe decline in the CMAP amplitude. In contrast, the CMAP amplitude decreased gradually and modestly in *SOD1-G93A* mice injected with the MuSK agonist antibody. After 5s, the MuSK agonist improved CMAP amplitude by 13.6% in females and by 31.7% in males (n=6-7; p<0.0001). The faint grey and blue lines indicate the SEMs. (C,D) 50Hz stimulation (S, arrow) of the phrenic nerve in *SOD1-G93A* mice injected with the control antibody to GP120 led to frequent failures (F, arrow) to elicit a

CMAP, whereas CMAPs were reliably elicited in *SOD1-G93A* mice injected with the MuSK agonist antibody, similar to the number of failures seen in wild-type mice. The MuSK agonist antibody reduced the number of failures by 88% in females and 70% in males during 1min of stimulation. The scatter plot shows the values for individual mice, as well as the mean values and SEM; \*  $p < 0.05$ , \*\*  $p < 0.01$ , \*\*\*  $p < 0.001$ . The baseline CMAP amplitude data are as follows: anti-GP120-treated males,  $5.95 \pm 1.14 \text{mV}$ ; MuSK agonist antibody-treated males,  $5.93 \pm 0.52 \text{mV}$ ; anti-GP120-treated females,  $4.95 \pm 0.54 \text{mV}$ ; MuSK agonist antibody-treated females,  $5.81 \pm 0.63 \text{mV}$ .

**Figure 6. Chronic dosing with the MuSK agonist antibody increases motor neuron survival and extends the lifespan of *SOD1-G93A* mice.**

(A) Representative images of lumbar spinal cords stained with antibodies to ChAT (scale bar=100 $\mu\text{m}$ ). (B) At P138, during the peak period of motor neuron cell death, the number of spinal motor neurons in the lumbar enlargement is greater in *SOD1-G93A* mice treated with the agonist antibody to MuSK (■) than in mice treated with the control

antibody to GP120 (●). The scatter plot shows the values for individual mice (n = 3 to 5), as well as the mean values and SEM; \* p<0.05, \*\* p<0.01, \*\*\* p<0.001. (C, D) Female and male *SOD1-G93A* mice chronically injected with the control antibody to GP120 have a life span of 169 and 157.5 days, respectively (dotted line). Chronic injection of the reverse chimera MuSK agonist antibody prolongs longevity by 7 and 10 days in female and male *SOD1-G93A* mice, respectively (solid line). n≥13; \* p<0.05, \*\* p<0.01, \*\*\*p<0.001.

### **Figure 1-figure supplement 1**

**MuSK agonist antibody #13 stimulates MuSK tyrosine phosphorylation *in vivo*.** (A) The MuSK agonist antibody (Ab #13) failed to stimulate MuSK phosphorylation in innervated (Inn) muscle, suggesting that MuSK may be maximally phosphorylated at synapses by Agrin and Lrp4. (B) Following denervation (Den), non-synaptic regions of muscle express MuSK, but not neural Agrin. Ab #13 stimulated MuSK phosphorylation in denervated muscle by 2.2-fold, demonstrating that Ab #13 activates MuSK *in vivo*. (C) Following denervation, MuSK expression increases 7.5-fold, but expression of Dok-7, an essential,

inside-out activator of MuSK, increases only 2.0-fold. Thus, the activity of Ab #13 in denervated muscle may be limited by low non-synaptic Dok-7 expression. (A, B) The ratio of MuSK-P/MuSK in the absence of Ab #13 was assigned a value of 1.0. (C) The level of MuSK and Dok-7 expression in innervated muscle was assigned a value of 1.0. The SEMs (n=3) are shown in (A, C); values and averages from two experiments are shown in (B).

### **Figure 3-figure supplement 1**

***hSOD1 G93A* copy number remained unchanged over generations and throughout the experiments.** (A) The copy number of the human *SOD1 G93A* gene was quantified by real-time PCR and normalized to *GAPDH*. All mice included in this study had 21-26 copies of *hSOD1 G93A*. The normalized *hSOD1 G93A* Ct values are shown for 25 samples (filled circles).

### **Figure 4-figure supplement 1**

**The human and reverse chimera versions of MuSK agonist antibody #13 induce acetylcholine receptor (AChR) clustering in C2C12 myotubes whereas a Fab from MuSK antibody #13 fails to stimulate**

**AChR clustering.** (A) Human (h) and reverse chimera (rc) MuSK #13 antibodies are similarly effective in stimulating AChR clustering in C2C12 myotubes (n=3). (B,C) C2C12 myotubes were treated with rc MuSK #13 or a Fab from MuSK #13 for 16 hr at the indicated concentrations and stained with  $\alpha$ -BGT. We found that the Fab fragment from antibody #13, unlike the intact IgG or the scFv, was unable to stimulate clustering of AChRs, indicating that antibodies must be dimeric and force-dimerize MuSK and promote an orientation that is favorable for trans-phosphorylation. (C) The rc antibody #13 stimulates AChR clustering in a dose-dependent and saturable manner, whereas Fab #13 fails to stimulate AChR clustering (n= 3).

#### **Figure 4-figure supplement 2**

**The reverse chimera MuSK agonist antibody #13 has a half-life of 11 days and chronic dosing with this antibody maintains the agonist antibody at levels that are sufficient to saturate MuSK at the synapse.** Rc MuSK antibody #13 was produced to minimize the occurrence of an immune response to a human antibody, as well as to eliminate the danger of eliciting an immune response at the

neuromuscular synapse. (A) Following a single 10mg/kg injection of reverse chimera MuSK agonist antibody #13 in wild-type mice, the amount of antibody in the blood decreased over time as a single exponential with a half-life of 11 days. (B) Repeated 10mg/kg injections of reverse chimera MuSK agonist antibody #13, every 24 days, in *SOD1 G93A* mice restored antibody levels and maintained the antibody at levels that were sufficient to saturate MuSK at the synapse. The mean values for individual mice (n=5) and the SEM are shown.

### **Figure 4-figure supplement 3**

**Chronic dosing with the MuSK agonist antibody increases the extent of nerve terminal coverage at partially innervated synapses in *SOD1 G93A* mice.** (A) The number (~50%) of partially innervated synapses in *SOD1 G93A* mice is not altered by chronic injection of reverse chimera MuSK agonist antibody #13 (■). The inset shows a representative partially innervated synapse (scale bar=20µm). (B) The extent of the AChR-rich postsynaptic membrane that is apposed by nerve terminals (NT) is greater in *SOD1 G93A* mice injected with the MuSK agonist antibody (■) than with a control antibody to GP120 (●).

The scatter plot shows the values for individual mice, as well as the mean values and SEM; \*  $p < 0.05$ , \*\*  $p < 0.01$ , \*\*\*\*  $p < 0.0001$ .

### **Figure 5-figure supplement 1**

**Drawing of experimental protocol to stimulate the phrenic nerve and record CMAPs in the diaphragm muscle.** The phrenic nerve was placed in a bipolar suction electrode for stimulation. CMAPs were recorded from a suction recording electrode placed in the same place (dotted circle) across the different animals used in this study. The phrenic nerve is shown in blue, the blood vessels in red and the area with acetylcholine receptors in grey.

<b>Reagent type.</b> Duplicate rows as needed. Order is flexible, but row titles must be preserved. <b>Species</b> (mandatory if applicable). Append in parentheses. First mention, use full genus. <b>Sex</b> (if applicable). Add within parentheses after species.	<b>Designation.</b> Symbol/name used in publication. Separate multiple entries with semi-colon, space. (If semi-colon within designation, delimit with double quotes.)	<b>Source (public).</b> Stock center, company, data repository. <b>Reference.</b> Include PMID or DOI; use "this paper" if new. <b>If neither</b> applies enter "other" and explain in Additional Information.	<b>Identifiers.</b> Format as <i>ID_source:identifier</i> . Separate multiple entries with semi-colon, space. Include catalog numbers, stock numbers, database IDs or accession numbers, RRDs.	<b>Additional information.</b> Mandatory if column C entry is "this paper" or "other". Description of new reagent; laboratory from which reagent obtained; other pertinent information. For antibodies, indicate dilution and conditions used.
<b>Key Resources Table</b>				
<b>Reagent type (species) or resource</b>	<b>Designation</b>	<b>Source or reference</b>	<b>Identifiers</b>	<b>Additional information</b>
gene ( )				
strain, strain background ( )	Mouse: B6.Cg-Tg(SOD1*G93A)1Gur/J	The Jackson Laboratory	RRID:IMSR_JAX:004435	
	Mouse: C57BL/6J	The Jackson Laboratory	RRID:IMSR_JAX000664	
genetic reagent ( )				
cell line ( )	Mouse C2C12 skeletal muscle cells	Burden lab	ATCC Cat# CRL-1772, RRID:CVCL_0188	
	Mouse: Immortalized wild-type muscle cells	Burden lab	PMID: 18848351	
	Mouse: Immortalized <i>Lrp4</i> mutant muscle cells	Burden lab	PMID: 18848351	
transfected construct ( )				
biological sample ( )				
antibody	Rabbit anti-Neurofilament-L	SYnaptic SYstems	Cat# 171 002, RRID:AB_887743	
	Rabbit anti-Synapsin 1/2	SYnaptic SYstems	Cat# 106 002, RRID:AB_887804	
	Alexa 647-anti-human IgG	Life Technologies	Cat# A-21445, RRID:AB_2535862	
	anti-Choline Acetyltransferase	Millipore	Cat# AB144P-200UL, RRID:AB_90661	
	anti-NeuN	Millipore	Cat# MAB377, RRID:AB_2298772	
	Rabbit anti-MuSK	Burden lab	PMID: 10781064	
	Goat anti-MuSK	R&D Systems	Cat# AF3904, RRID:AB_2147242	
	Rabbit anti-Dok-7	Burden lab	PMID: 18848351	
	Mouse anti-phosphotyrosine 4G10	Millipore		
recombinant DNA reagent				
sequence-based reagent				

peptide, recombinant protein	Alexa 594-alpha-bungarotoxin	Life Technologies	Cat#B13423	
	Alexa 488-alpha-bungarotoxin	Life Technologies	Cat#B13422	
	Hoechst 33342	Thermo Fisher	Cat# 62249	
	Recombinant Rat Agrin Protein	R&D Systems	Cat#550-AG-100	
commercial assay or kit	GAPDH TaqMan Assay Mm00186822_cn	Thermo Fisher	Cat# 4400291	
chemical compound, drug				
software, algorithm	Prism 7.0	<a href="http://www.graphpad.com/scientific-software/prism/">http://www.graphpad.com/scientific-software/prism/</a>	RRID:SCR_002798	
	Volocity 3D Image Analysis Software	<a href="http://www.perkinelmer.com/pages/020/cellularimaging/products/volocity.xhtml">http://www.perkinelmer.com/pages/020/cellularimaging/products/volocity.xhtml</a>	RRID:SCR_002668	
	pCLAMP Software Suite	<a href="https://www.moleculardevices.com/systems/axon-conventional-patch-clamp/pclamp-11-software-suite">https://www.moleculardevices.com/systems/axon-conventional-patch-clamp/pclamp-11-software-suite</a>		
other	DietGel 76A	ClearH20	Cat#72-07-5022	

Fig. 1

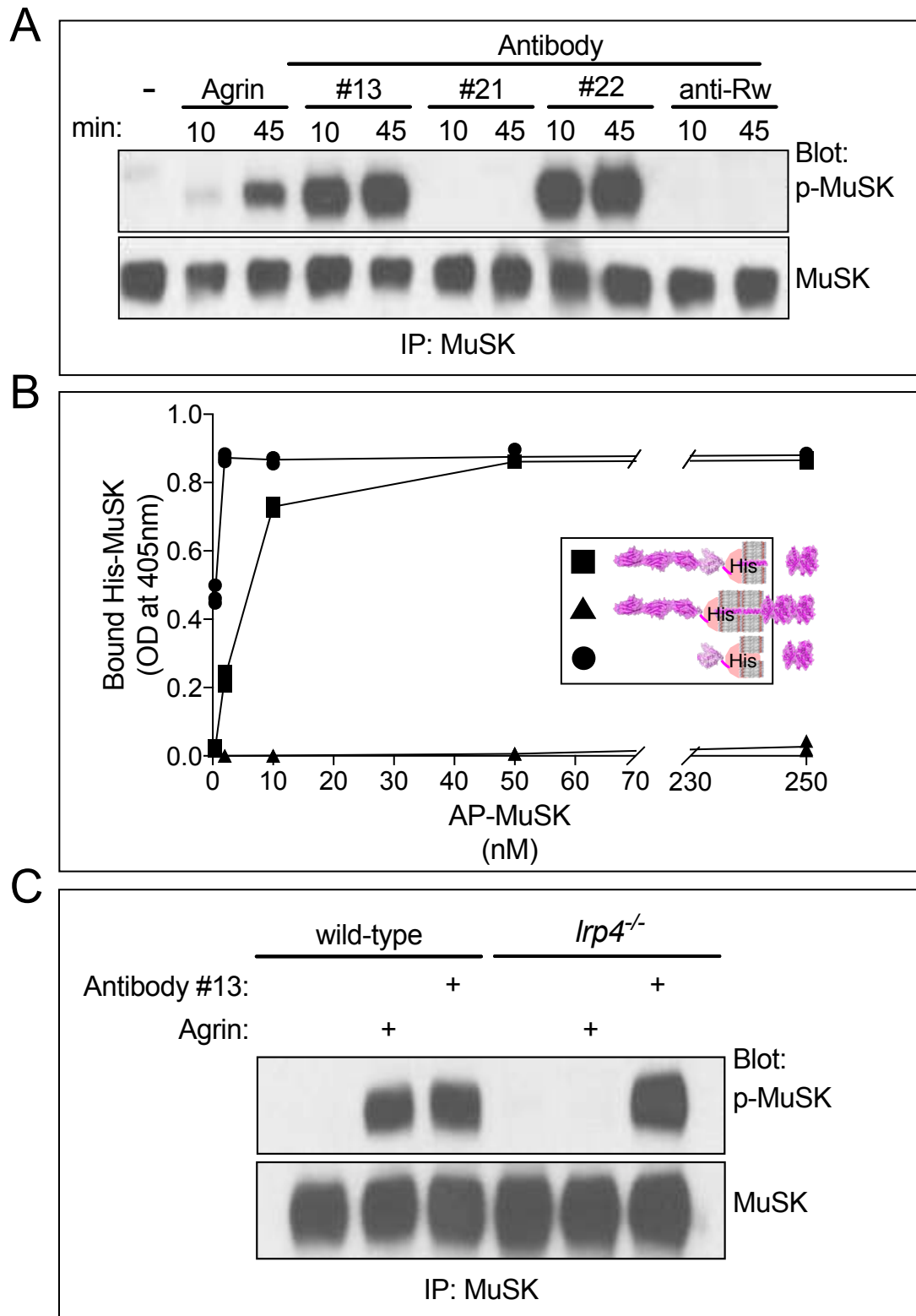


Fig. 2

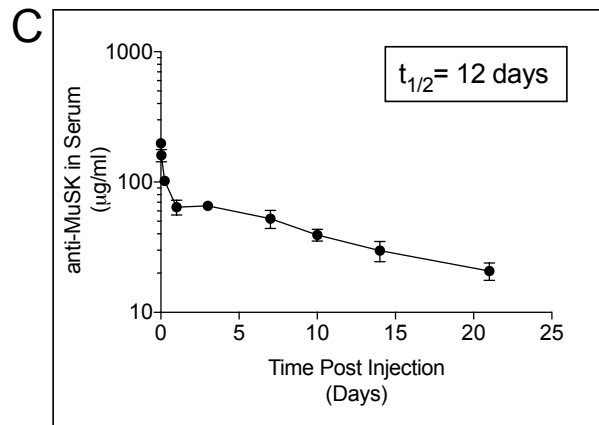
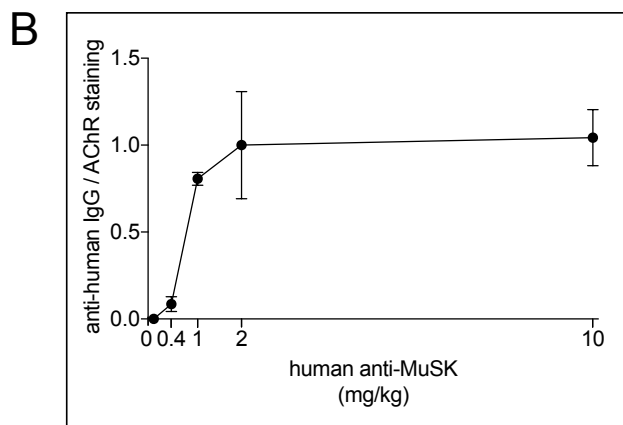
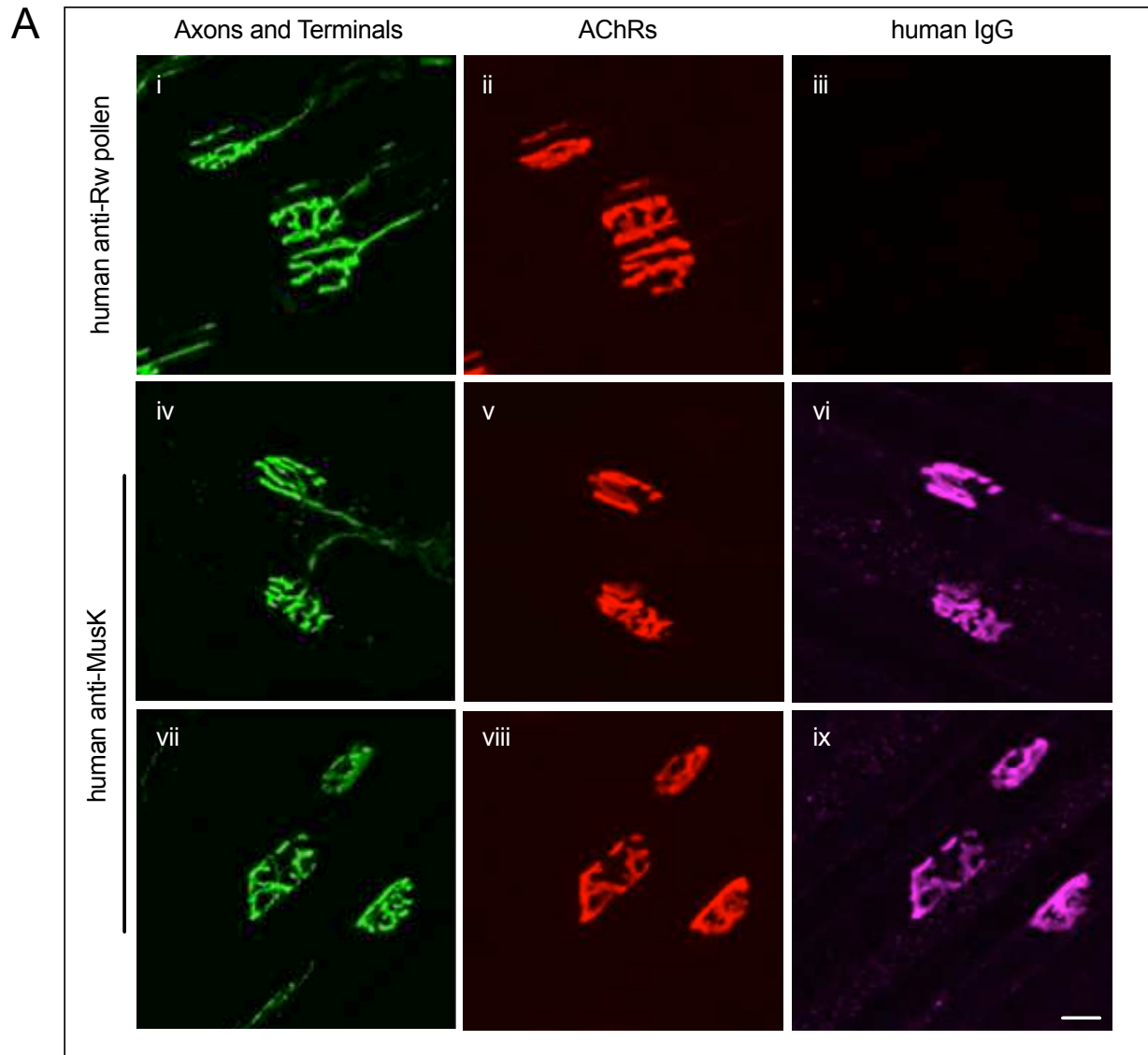


Fig. 3

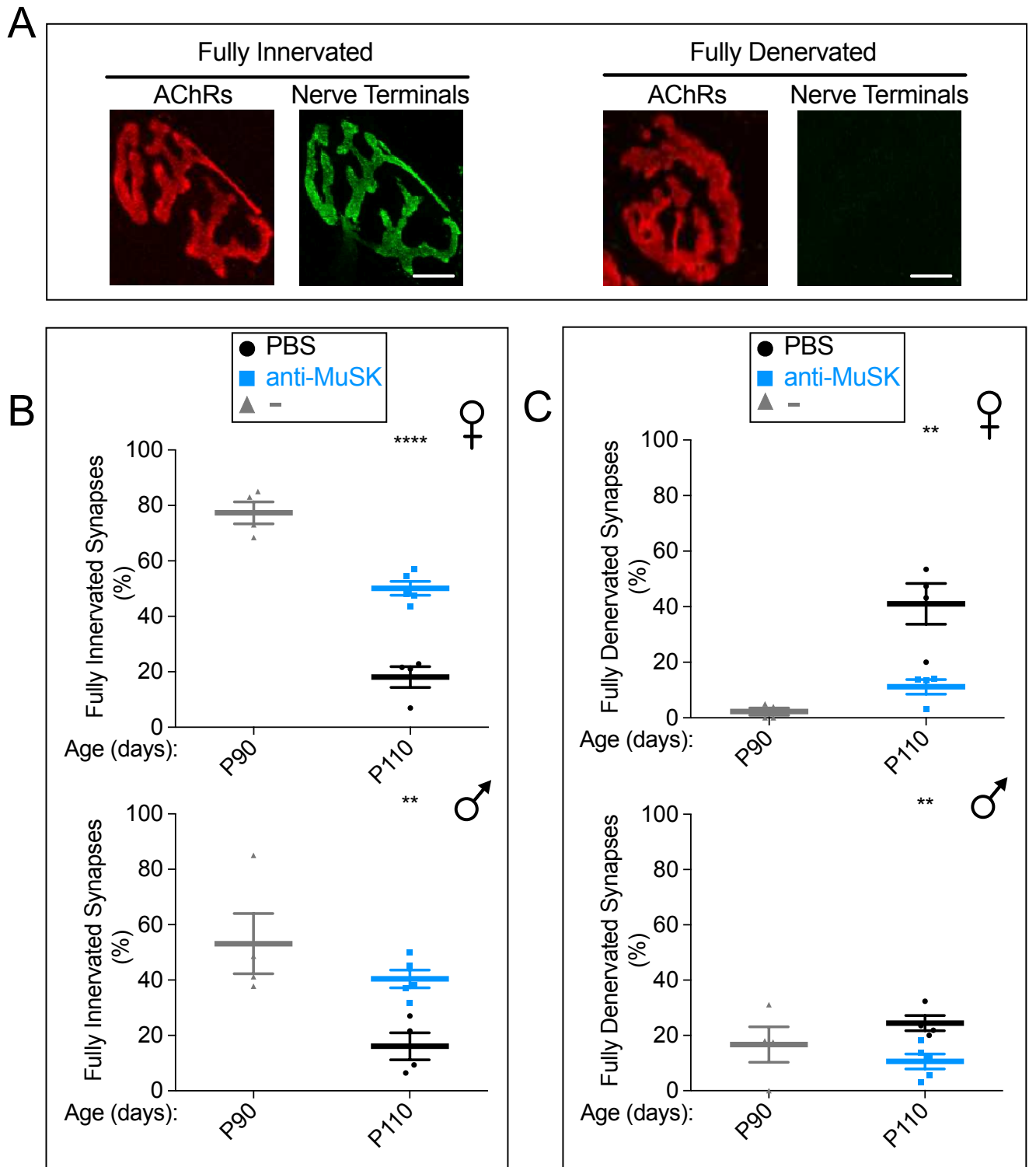


Fig. 4

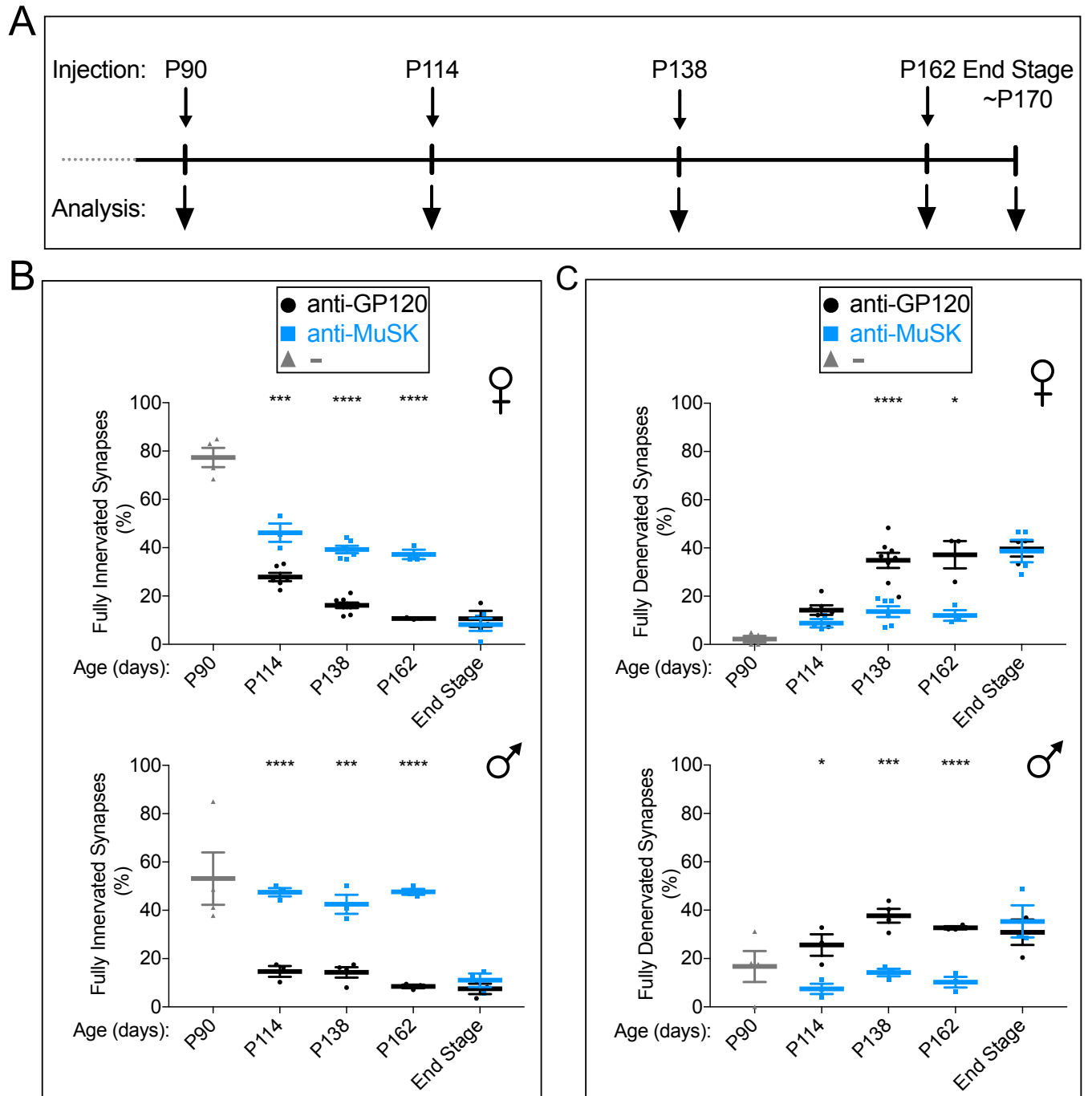


Fig. 5

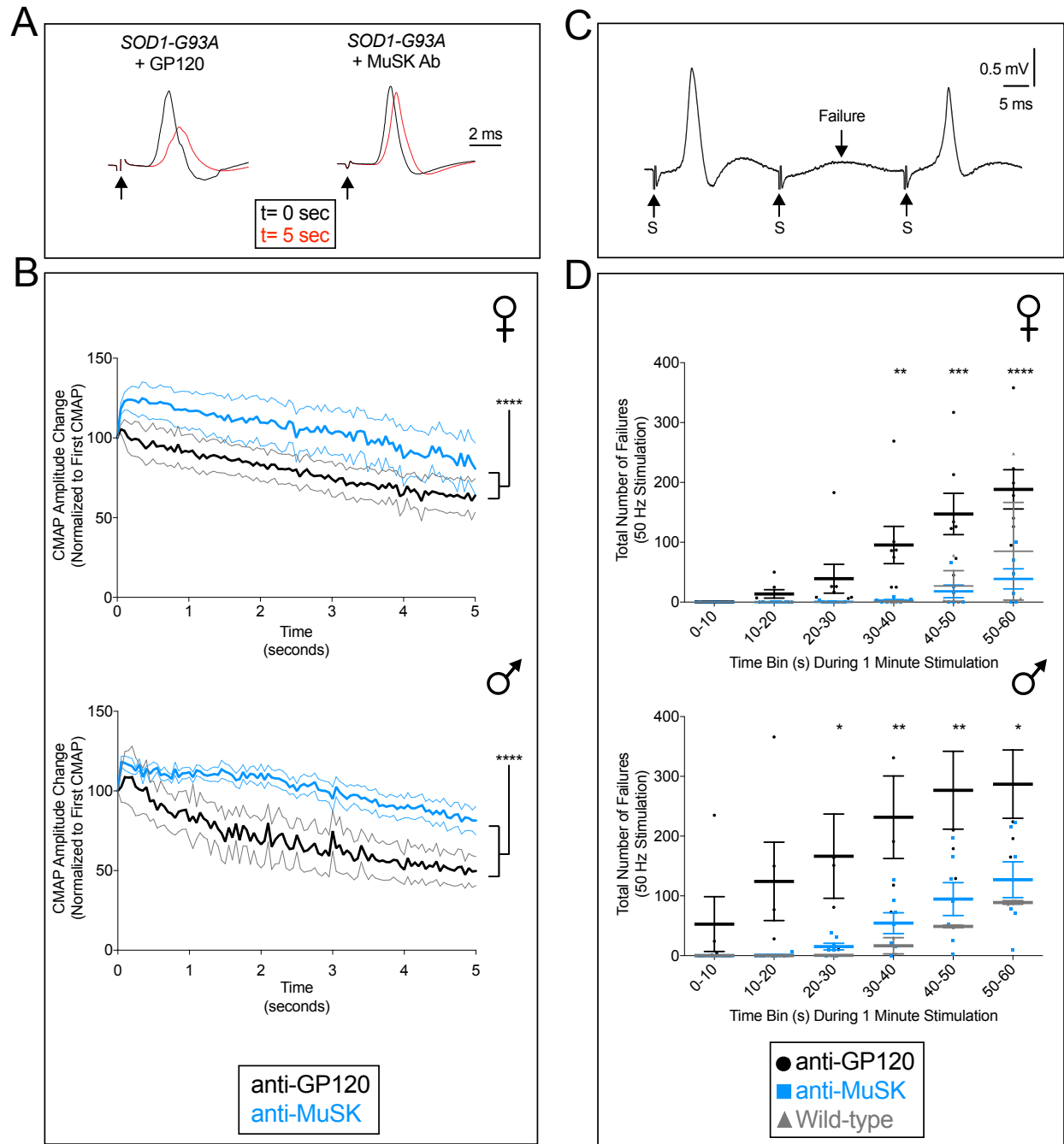
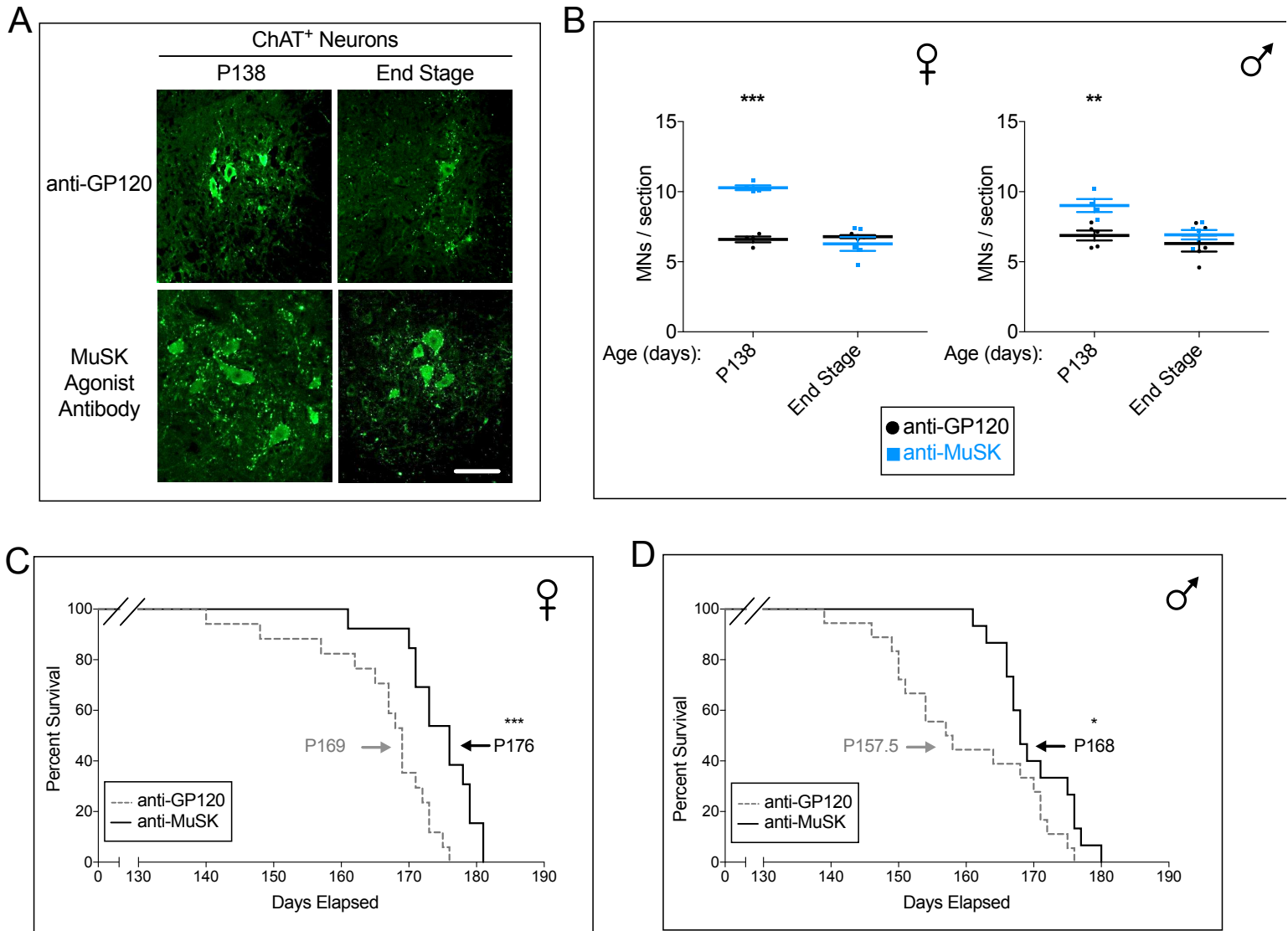
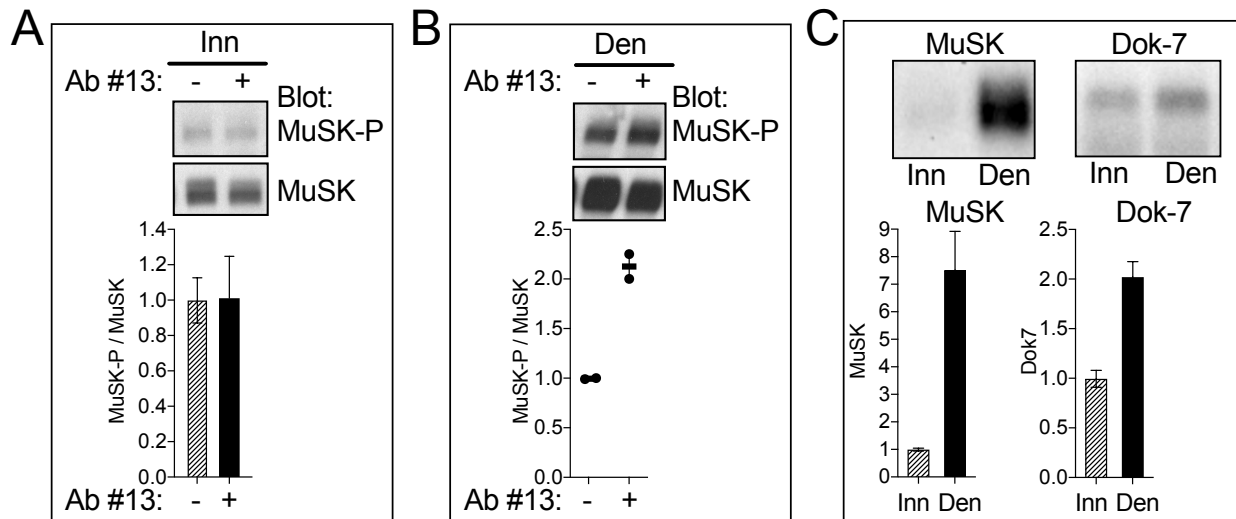


Fig. 6



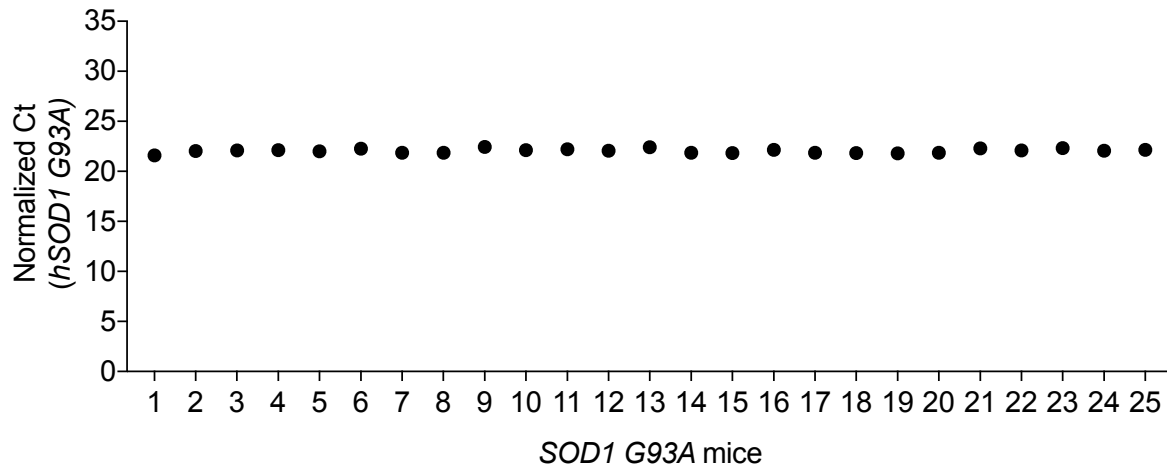
## Figure 1- Figure Supplement 1



**MuSK agonist antibody #13 stimulates MuSK tyrosine phosphorylation *in vivo*.** (A) The MuSK agonist antibody (Ab #13) failed to stimulate MuSK phosphorylation in innervated (Inn) muscle, suggesting that MuSK may be maximally phosphorylated at synapses by Agrin and Lrp4. (B) Following denervation (Den), non-synaptic regions of muscle express MuSK, but not neural Agrin. Ab #13 stimulated MuSK phosphorylation in denervated muscle by 2.2-fold, demonstrating that Ab #13 activates MuSK *in vivo*. (C) Following denervation, MuSK expression increases 7.5-fold, but expression of Dok-7, an essential, inside-out activator of MuSK, increases only 2.0-fold. Thus, the activity of Ab #13 in denervated muscle may be limited by low non-synaptic Dok-7 expression. (A, B) The ratio of MuSK-P/MuSK in the absence of Ab #13 was assigned a value of 1.0. (C) The level of MuSK and Dok-7 expression in innervated muscle was assigned a value of 1.0. The SEMs (n=3) are shown in (A, C); values and averages from two experiments are shown in (B).

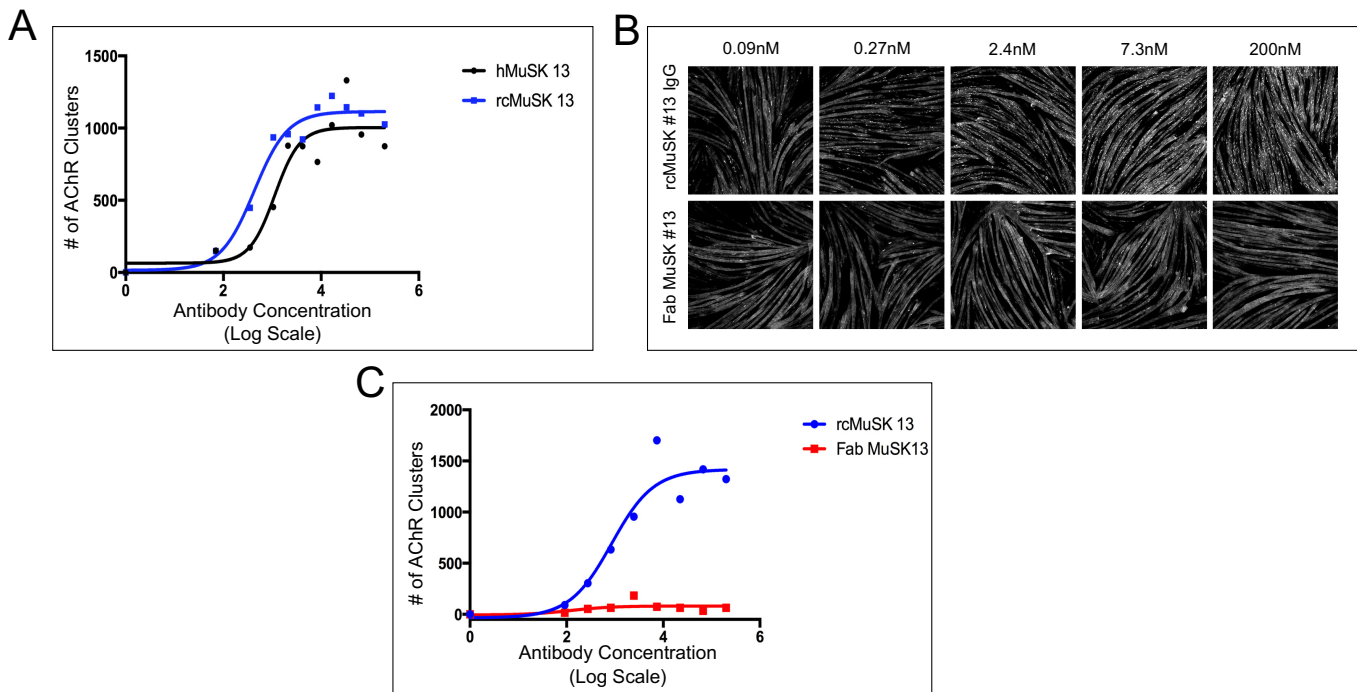
**Figure 3 - Figure Supplement 1**

**A**



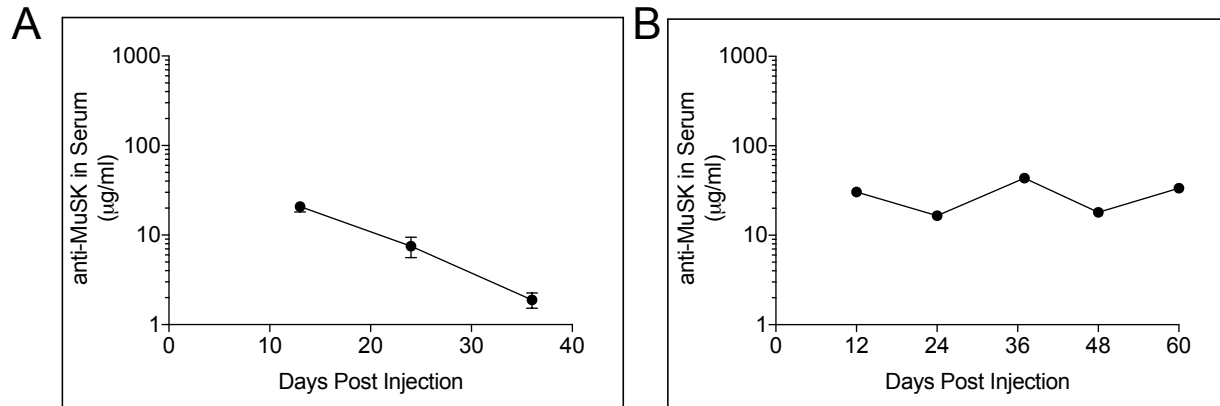
***hSOD1 G93A* copy number remained unchanged over generations and throughout the experiments.** (A) The copy number of the human *SOD1 G93A* gene was quantified by real-time PCR and normalized to *GAPDH*. All mice included in this study had 21-26 copies of *hSOD1 G93A*. The normalized *hSOD1 G93A* Ct values are shown for 25 samples (filled circles).

## Figure 4- Figure Supplement 1



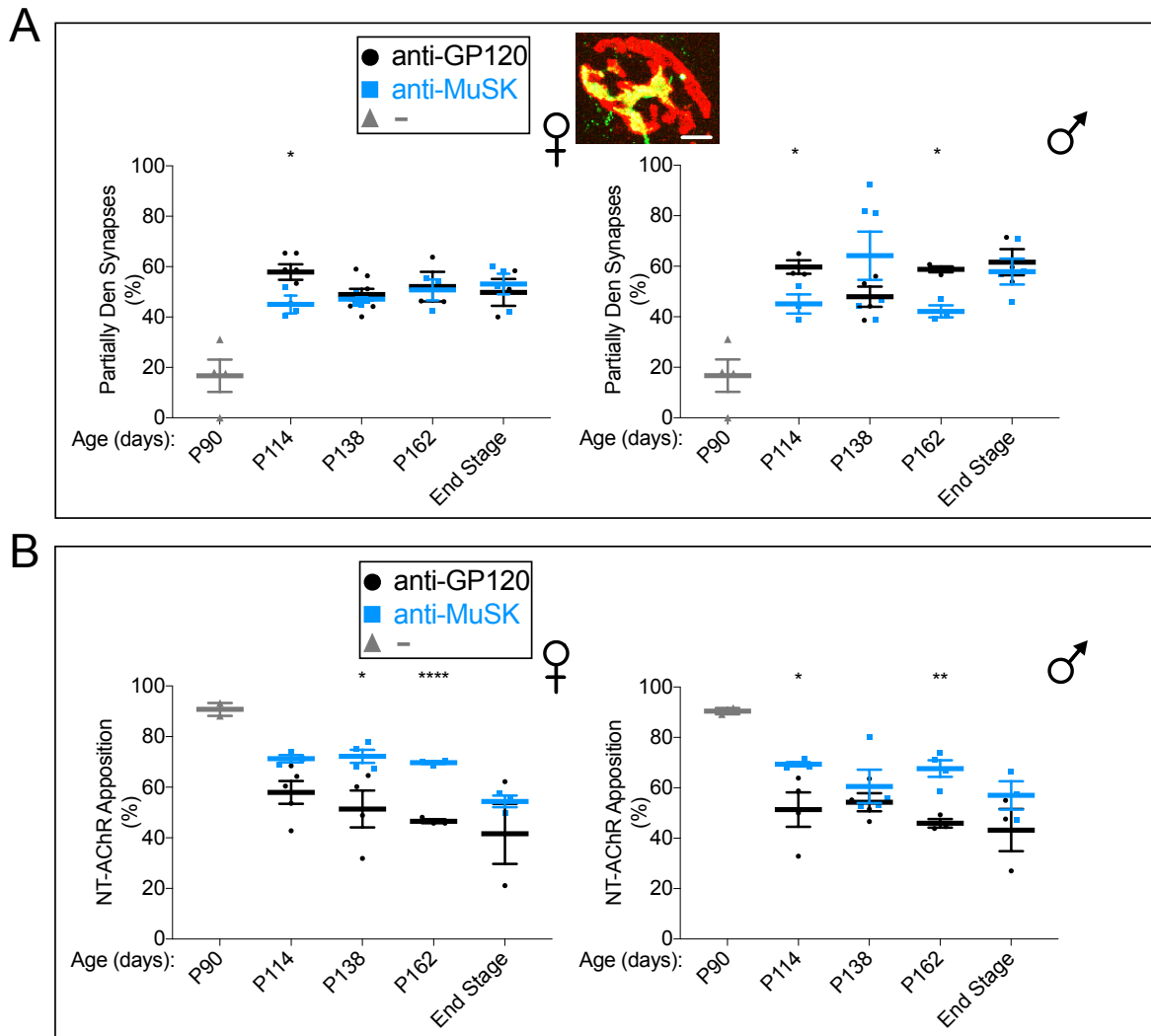
**The human and reverse chimera versions of MuSK agonist antibody #13 induce acetylcholine receptor (AChR) clustering in C2C12 myotubes whereas a Fab from MuSK antibody #13 fails to stimulate AChR clustering.** (A) Human (h) and reverse chimera (rc) MuSK #13 antibodies are similarly effective in stimulating AChR clustering in C2C12 myotubes (n=3). (B,C) C2C12 myotubes were treated with rc MuSK #13 or a Fab from MuSK #13 for 16 hr at the indicated concentrations and stained with  $\alpha$ -BGT. We found that the Fab fragment from antibody #13, unlike the intact IgG or the scFv, was unable to stimulate clustering of AChRs, indicating that antibodies must be dimeric and force-dimerize MuSK and promote an orientation that is favorable for trans-phosphorylation. (C) The rc antibody #13 stimulates AChR clustering in a dose-dependent and saturable manner, whereas Fab #13 fails to stimulate AChR clustering (n= 3).

**Figure 4- Figure Supplement 2**



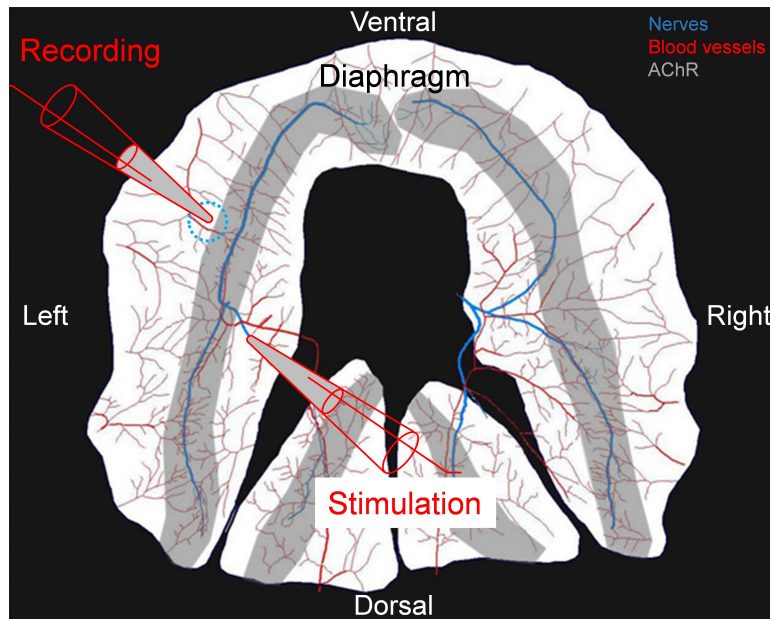
**The reverse chimera MuSK agonist antibody #13 has a half-life of 11 days and chronic dosing with this antibody maintains the agonist antibody at levels that are sufficient to saturate MuSK at the synapse.** Rc MuSK antibody #13 was produced to minimize the occurrence of an immune response to a human antibody, as well as to eliminate the danger of eliciting an immune response at the neuromuscular synapse. (A) Following a single 10mg/kg injection of reverse chimera MuSK agonist antibody #13 in wild-type mice, the amount of antibody in the blood decreased over time as a single exponential with a half-life of 11 days. (B) Repeated 10mg/kg injections of reverse chimera MuSK agonist antibody #13, every 24 days, in *SOD1 G93A* mice restored antibody levels and maintained the antibody at levels that were sufficient to saturate MuSK at the synapse. The mean values for individual mice (n=5) and the SEM are shown.

**Figure 4- Figure Supplement 3**



**Chronic dosing with the MuSK agonist antibody increases the extent of nerve terminal coverage at partially innervated synapses in *SOD1 G93A* mice.** (A) The number (~50%) of partially innervated synapses in *SOD1 G93A* mice is not altered by chronic injection of reverse chimera MuSK agonist antibody #13 (■). The inset shows a representative partially innervated synapse (scale bar=20 $\mu$ m). (B) The extent of the AChR-rich postsynaptic membrane that is apposed by nerve terminals (NT) is greater in *SOD1 G93A* mice injected with the MuSK agonist antibody (■) than with a control antibody to GP120 (●). The scatter plot shows the values for individual mice, as well as the mean values and SEM; \*  $p < 0.05$ , \*\*  $p < 0.01$ , \*\*\*  $p < 0.0001$ .

**Figure 5- Figure Supplement 1**



**Drawing of experimental protocol to stimulate the phrenic nerve and record CMAPs in the diaphragm.** The phrenic nerve was placed in a bipolar suction electrode for stimulation. CMAPs were recorded from a suction recording electrode placed in the same place (dotted circle) across the different animals used in this study. The phrenic nerve is shown in blue, the blood vessels in red and the area with acetylcholine receptors in grey.